CCS Chemistry

RESEARCH ARTICLE

Received: June 3, 2020 | Accepted: July 15, 2020

Positive/Negative Phototropism: Controllable Molecular Actuators with Different Bending Behavior

Haoran Wang[1,2], Jiapeng Liu[3], Kaiqi Ye[1], Qiyao Li[2], Jianyu Zhang[2], Hao Xing[2], Peifa Wei[2], Jingbo Sun[1], Francesco Ciucci[3,4], Jacky W. Y. Lam[2], Ran Lu[1]* & Ben Zhong Tang[2]*

[1]*State Key Laboratory of Supramolecular Structure and Materials, College of Chemistry, Jilin University, Changchun,* [2]*Department of Chemistry, Hong Kong Branch of Chinese National Engineering Research Center for Tissue Restoration and Reconstruction, Institute for Advanced Study, The Hong Kong University of Science and Technology, Hong Kong,* [3]*Department of Mechanical and Aerospace Engineering, The Hong Kong University of Science and Technology, Hong Kong,* [4]*Department of Chemical and Biomolecular Engineering, The Hong Kong University of Science and Technology, Hong Kong*

**Corresponding authors: luran@mail.jlu.edu.cn; tangbenz@ust.hk*

Cite this: *CCS Chem*. **2020**, *2*, 1491–1500

Herein, a series of molecular actuators based on the crystals of (*E*)-2-(4-fluorostyryl)benzo[*d*]oxazole (BOAF4), (*E*)-2-(2,4-difluorostyryl)benzo[*d*]oxazole (BOAF24), (*E*)-2-(4-fluorostyryl)benzo[*d*]thiazole (BTAF4), and (*E*)-2-(2,4-difluorostyryl)benzo[*d*]thiazole (BTAF24) showed unique bending behavior under UV irradiation. The one-dimensional (1D) crystals of BOAF4 and BTAF4 bent toward light, whereas those of BOAF24 and BTAF24 bent away from light. Although the chemical structures of these compounds are similar, the authors found that F···H–C interaction played a key role in the different molecular packing in structures crystals, which led to the positive/negative phototropism of the actuators. Moreover, theoretical calculations were carried out to reveal the mechanical properties of the crystals. Taking advantage of these photomechanical properties, the authors achieved the potential application in pushing objects, as well as enriching and removing pollutants. Hence, the molecular actuators with different bending behavior could be fabricated by introducing different number of F atom, which may open a novel gate for crystal engineering.

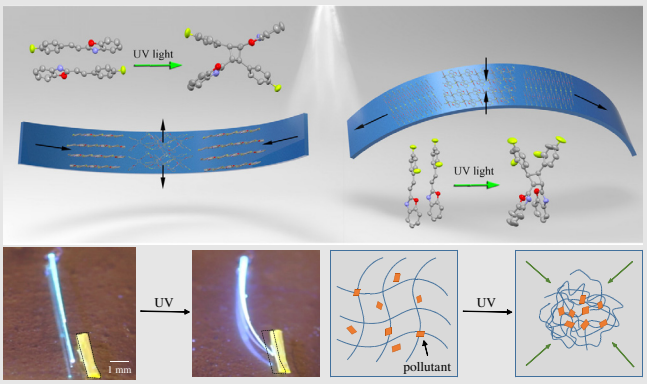

Keywords: **crystal engineering, actuators, phototropism, [2 + 2] cycloaddition, photomechanical effects**

Introduction

Nature endows organisms with tropisms for moving toward or away from a stimulus. For most plants, their stem exhibits positive phototropism to maximize photosynthetic energy for promoting growth.[1,2] However, most roots and some vine shoot tips exhibit negative phototropism, allowing them to grow toward darkness, drill into the soil, and climb objects.[3] The combination of positive and negative phototropism allows plants to grow in the correct direction, to make better use of light energy. Inspired by the response of natural organisms to external

DOI: 10.31635/ccschem.020.202000350
CCS Chem. **2020**, *2*, 1491–1500

stimuli, various artificially intelligent materials, such as artificial muscles and flexible electronics, have been developed.[4-10] Among them, photomechanical responsive materials have emerged as a research hot spot with unique advantages, including easy-to-achieve remote control and the miniaturization of devices.[11,12] Especially, photomechanical molecular crystals exhibit some conspicuous merits over polymer-based materials, such as faster response time,[13] higher Young's modulus,[14] and an ordered crystal structure that can be easily characterized by X-ray diffraction (XRD) techniques.[6] In addition, an ordered crystal structure offers opportunities for rapid energy transfer between tightly packed molecules, and this could be used as a physical platform for actuation from the nanoscale to the macroscale.[15,16] It has been found that the crystals based on photochemical active organic compounds, including azobenzenes, anthracenes, diarylethenes, and furylfulgides, are capable of bending,[17-30] curling,[31] twisting,[31,32] crawling,[33-37] and leaping[5,38] in response to light.

Recently, Naumov et al.[39] reported that a smart cocrystal of probenecid and 4,4′-azopyridine, which could reversibly respond to multiple external stimuli (heat, UV light, and mechanical pressure) by twisting, bending, and elastic deformation without fracture. Bardeen et al.[40] reported that the controllable movement of molecular crystals based on 1,2-bis(2-methyl-5-phenyl-3-thienyl) perfluorocyclopentene by varying the angle of incident light. As far as we know, previous efforts to regulate the motion behavior of crystals mainly focused on changing external conditions such as controlling the crystal habits and the irradiation direction. Till now, controlling the motion modes such as positive and negative phototropism through tuning crystal structure has posed a significant challenge.

In our previous work, we found that the introduction of chlorine at different position of benzene in styrylbenzoxazoles could affect the molecular packing structures in the crystals, which would further affect the topophotochemical reaction.[41] Compared with chlorine, fluorine possesses a smaller atomic radius and a stronger electronegativity, so introducing fluorine into conjugated organic molecules might lead to a unique arrangement in crystals and interesting photomechanical behavior. With these considerations in mind, we intended to study the photoinduced mechanical motions of the molecular crystals based on fluorine-containing styrylbenzoxazoles [(*E*)-2-(4-fluorostyryl)benzo[*d*]oxazole (**BOAF4**) and (*E*)-2-(2,4-difluorostyryl)benzo[*d*]oxazole (**BOAF24**)] and styrylbenzothiazoles [(*E*)-2-(4-fluorostyryl)benzo[*d*]thiazole (**BTAF4**) and (*E*)-2-(2,4-difluorostyryl)benzo[*d*]thiazole (**BTAF24**); Scheme 1] so as to reveal the effect of the molecular structures and crystal habits on photomechanical behavior. It was found that the crystals of **BOAF4**, **BOAF24**, **BTAF4**, and **BTAF24** with different habits showed photoinduced bending, curling, fragmentation, swelling, and photosalient behavior. Interestingly, the crystals of **BOAF4** and **BTAF4** showed photoinduced bending toward light, but the crystals of **BTAF4** and **BTAF24** showed oppositely photoinduced bending away from light.

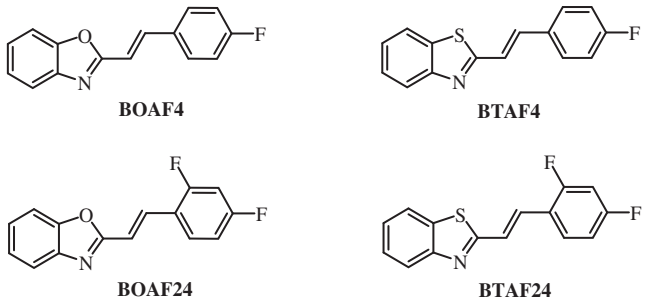

Scheme 1 | *Molecular structures of fluorine-containing styrylbenzoxazoles and styrylebenthiazoles.*

Experimental Methods

General information

^{1}H NMR and ^{13}C NMR spectra were recorded with a Mercury plus instrument (Varian. Palo Alto, California, USA) at 400 and 101 MHz using deuterated chloroform ($CDCl_3$) and deuterium dimethyl sulfoxide (DMSO-d_6) as the solvents. Fourier transform infrared (FT-IR) spectra were obtained with a Nicolet-360 FT-IR (Thermo Scientific, Middlesex County, Massachusetts, USA) spectrometer by the incorporation of samples into potassium bromide (KBr) disks. Mass spectra were measured with an AXIMA CFR matrix-assisted laser desorption/ionization time-of-flight (MALDI-TOF) mass spectrometer (compact, Shimadzu, Kyoto, Japan). The UV–Vis absorption spectra were obtained using a Mapada UV-1800pc spectrophotometer (Shimadzu, Kyoto, Japan). Fluorescence emission spectra were taken on a Cary Eclipse fluorescence spectrophotometer (Agilent, Santa Clara, California, USA). Fluorescence microscopy images were taken on a Fluorescence Microscope (Olympus Reflected Fluorescence System BX51, Olympus, Japan). XRD patterns were obtained on an Empyrean XRD (Malvern Instruments, London, UK), equipped with graphite monochromatized Cu-Kα radiation (λ = 1.5418 Å), employing a scanning rate of 0.00267°s^{-1} in the 2θ range of 2°–40°. The single crystals of **BTAF4** and **BTAF24** were obtained by slow evaporation from the solutions in dichloromethane (CH_2Cl_2)/petroleum ether (v/v = 1/4). The photodimerization products of **D-BTAF4** and **D-BTAF24** were gained via irradiating the microcrystals of **BTAF4** and **BTAF24** under 365 nm for 30 min, followed by recrystallization from petroleum ether. The single crystals of **D-BTAF4** and **D-BTAF24** were obtained in CH_2Cl_2 under petroleum ether steam by the vapor

DOI: 10.31635/ccschem.020.202000350
CCS Chem. **2020**, *2*, 1491–1500

diffusion method. The above single crystals were selected for XRD analysis on an APEX II diffractometer (Bruker, Middlesex County, Massachusetts, USA), using graphite-monochromated Mo-Kα radiation (λ = 0.71073 Å). The structures were solved by the direct methods and refined on F2 by full-matrix least-squares using the SHELXTL-97 program (George M. Sheldrick, Thomas R. Schneider, Lower Saxony, Germany). The non-hydrogen atoms (S, C, N, and F) were easily placed from the subsequent Fourier difference maps and refined anisotropically. The H atoms were introduced in the calculated positions and refined with fixed geometry with respect to their carrier atoms. Cambridge Crystallographic Data Centre (CCDC) 1814131, 1814889, 1850307, and 1850304 contain the supplementary crystallographic data for **BTAF4**, **BTAF24**, **D-BTAF4**, and **D-BTAF24**, respectively. The single-crystal data for **BOAF4**, **BOAF24**, **D-BOAF4**, and **D-BOAF24** can be found in our previous work.[42] Photomechanical behaviors were observed under a microscope, and the crystals were put on the glass substrate and irradiated by pocket lamp (365 nm, 3 W) for different times at 298 K. **BOAF24** fibers were obtained by dropping the solution in tetrahydrofuran (THF; 1.0 × 10^{-2} mol/L) into sodium dodecyl sulfate aqueous solution (2 mg/mL) under stirring.

THF was dried over sodium and benzophenone. CH_2Cl_2 was dried over calcium hydride. The other reagents were used without further purification.

Computational methods

We performed all the spin-unpolarized first-principle calculations using the Vienna ab initio simulation package (VASP, Vienna, Austria)[43,44] with plane-wave basis set and a projector-augmented wave (PAW) approach.[45] The exchange correlation is described using Perdew–Burke–Ernzerhof (PBE) functional[46] under the generalized gradient approximation (GGA) scheme. To obtain an accurate elastic constant, we set the kinetic energy cutoff as large as 700 eV and sampled the Brillouin zone using Gamma-centered *k*-meshes with at least 5000 k points per reciprocal atom (pra). The structures were first fully relaxed to ensure that the energy difference in each self-consistent calculation (SCF) was smaller than 10^{-6} eV, and the maximum force was converged below 0.005 eV/Å. The elastic tensor was then calculated based on the fully relaxed structure by performing two magnitudes of displacement (0.01 and –0.01 Å) for each atom along each of the Cartesian directions. The bulk modulus and shear modulus were finally calculated based on the converged elastic stiffness tensor.[47]

Synthesis

The syntheses of **BOAF4**, **BOAF24**, and **BTAF24** were reported previously.[41,48] **BTAF4** was synthesized according to the reported procedure.[41] The synthetic route and characterization data were shown in the Supporting Information.

Results and Discussion

Photomechanical behavior

First, the slice-like crystals and rod-like crystals of **BOAF4** were obtained from petroleum ether/CH_2Cl_2 (v/v = 3/1) in one test tube. In the case of the slice-like crystal with a low aspect ratio, the photoinduced swinging and swelling were observed (Supporting Information Figure S1 and Video S1). Accompanied by the photomechanical effect, the emission of **BOAF4** in crystal became stronger and blue-shifted gradually.[42] The thinner slice-like crystal displayed a different behavior, that it could bend toward UV light (Supporting Information Video S2 and Figure S2).

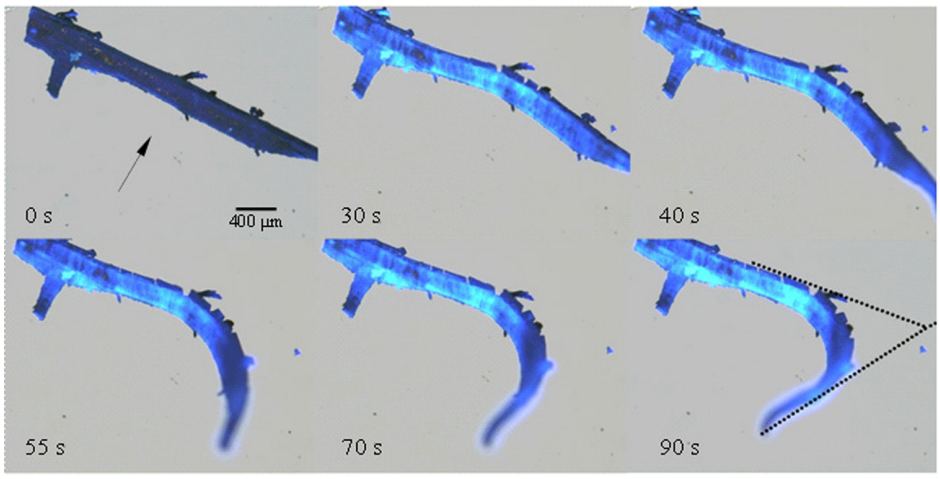

Figure 1. | *Optical photographs of the irregular rod-like crystal of **BOAF4** before and after irradiation vertically with 365-nm light for different time (the arrow indicates the irradiation direction).*

DOI: 10.31635/ccschem.020.202000350
CCS Chem. **2020**, *2*, 1491–1500

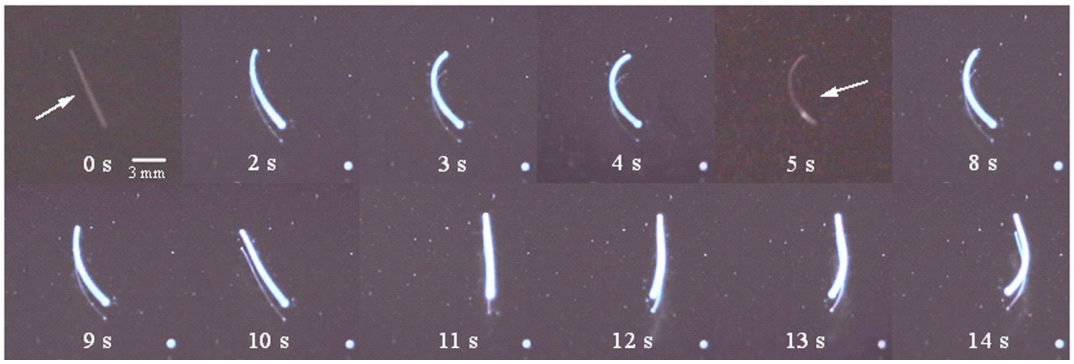

Figure 2. | *Optical photographs of rod-like crystals of **BOAF24** before and after irradiation with 365-nm light for different time (the arrows indicate the irradiation direction).*

Interestingly, for the irregular rod-like crystal of **BOAF4** with high aspect ratio, comparable bending behavior was observed under UV irradiation. Besides exhibiting photoinduced swelling, it could roll up its tail and bend toward the UV light (Figure 1 and Supporting Information Video S3). In detail, the UV irradiation induced the emergence of cracks in the backlight side of the crystal, and the tail bent toward light. When the irradiation time was prolonged to 90 s, the tail was raised out of the plane, and the bending angle was ca. 135° without break.

Therefore, **BOAF4** crystals with smaller thicknesses or high aspect ratios tend to bend toward a light source. Notably, in our previous work, the needle-like crystals of (*E*)-2-(2,4-dichlorostyryl)benzo[*d*]oxazole (**BOACl24**) bent away from the UV light,[41] opposite to the rod-like crystals of **BOAF4**. To further research the positive and negative phototropism behavior of crystals under UV irradiation, **BOAF24** was designed and synthesized for comparison with **BOAF4**.[48]

BOAF24 formed block, ribbon-like, and rod-like crystals in petroleum ether/CH_2Cl_2 (v/v = 3/1). The long block irregular crystal of **BOAF24** could swing upon UV irradiation, and small pieces jumped away from the body. When prolonging the UV irradiation, more cracks were observed in the cross sections of the crystal (Supporting Information Video S4). We also observed the energy accumulation state in the photomechanical process that Naumov et al.[6] proposed. As shown in Supporting Information Video S5, after turning off the UV lamp at 23 s, the crystal of **BOAF24** lay still at that time but began to break after 1 s. This proves that the photosalient behavior occurs after an induction period during which energy accumulates. Furthermore, the 1D crystal bent away from irradiation and the thinner crystals markedly exhibited more significant bending compared with the thicker ones (Supporting Information Video S6 and Figure S3a). When the crystals were vertically irradiated by UV light from the downside, the right side of the elongated crystal marked by the red circle bent up and could also bend down via turning around the irradiation direction. Meanwhile, the crystal part marked with the yellow circle gave a slight movement as it was thicker. Also, the bouquet-like crystals consisting of lots of ribbons displayed similar behavior (Supporting Information Figure S3b). Except for the bending behavior, the bouquet of ribbon-like crystals of **BOAF24** could even jump under UV irradiation (Supporting Information Video S7). To clearly observe the bending direction of the crystals, one rod-like crystal of **BOAF24** was selected. As shown in Supporting Information Video S8 and Figure 2, it clearly bent away from the light source upon being irradiated vertically by 365-nm light. When the irradiation direction was reversed, the bent crystal straightened. Prolonging the irradiation time, the crystal jumped at 11 s and continued to bend backward toward UV light. Such bending away from the light source was repeated several times, meaning that the photoinduced bending process is reversible.

For deep understanding of the different photomechanical effects of **BOAF4** and **BOAF24**, the crystals of their analogs **BTAF4** and **BTAF24** were obtained. As anticipated, a rod-like crystal of **BTAF4** bent toward UV light, and the bent crystal could be straightened when the irradiation direction was changed to the right side (Figure 3). Meanwhile, the enhanced fluorescence intensity was also observed (Supporting Information Figure S4).[49–51] We also obtained the rod-like, block, and slice-like crystals of **BTAF24** from cyclohexane/CH_2Cl_2 (v/v = 4/1). Under UV irradiation, the rod-like and slice-like crystals bent away from the light source, whereas the block crystals just jumped without any bending. As shown in Supporting Information Figure S5, after irradiation with 365-nm light from upside vertically, the straight rod-like crystal bent backward toward the light source. When the irradiation direction changed to the downside, the bent crystal could be straightened and further bent upward by prolonging the irradiation time. The backward bending of UV light was repeated several times (Supporting Information Video S9). The microcrystals of

DOI: 10.31635/ccschem.020.202000350
CCS Chem. **2020**, *2*, 1491–1500

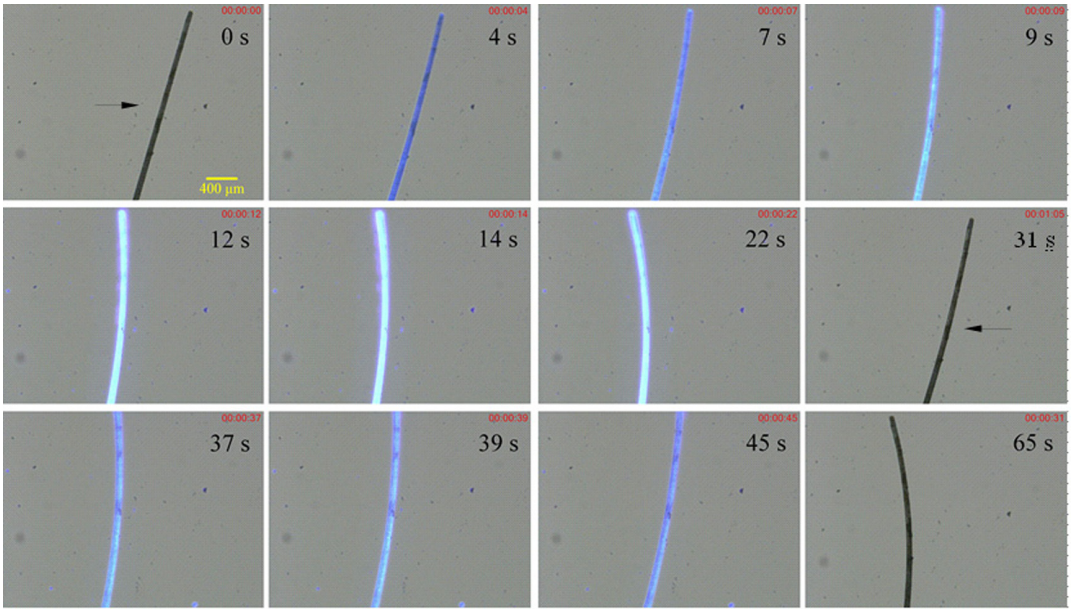

Figure 3. | *Optical photographs of the rod-like crystals of **BTAF4** before and after irradiation with 365-nm light for different time (the arrows indicate the irradiation directions).*

BTAF24 also showed "turn on" emission under UV irradiation (Supporting Information Figure S6). Furthermore, the block crystals of **BTAF24** could jump away from their original positions when the UV irradiation time was 3 s, and small pieces exploded out of the body (Supporting Information Video S10). The slice-like crystal of **BTAF24** bent backward toward the light source in the beginning of the irradiation, followed by splitting into several parts perpendicular to the long axis of the crystal (Supporting Information Video S11).

Mechanism study

In our previous work, we found that a photoinduced [2 + 2] cycloaddition reaction took place in the molecular crystals of **BOAF4** and **BOAF24**, which was the driving force for the photomechanical effects. Particularly, in the process of photoinduced movement, the crystals of **BOAF4** and **BOAF24** were "turned on" from nonemissive to emissive. **BOAF4** and **BOAF24** were typical aggregation-caused quenching (ACQ) molecules,[42] so the crystals were nonemissive before UV irradiation. Although the photodimerization broke the molecular conjugation to some extent, the intensified emission of the crystals of **BOAF4** and **BOAF24** was observed upon UV irradiation due to the intramolecular and intermolecular through-space conjugation.[42] Moreover, ^{1}H NMR spectral changes of **BTAF24** before and after UV irradiation for different times suggested that photodimerization occurred in the microcrystals. As depicted in Supporting Information Figure S7, after irradiating the microcrystals of **BTAF24** with UV light for 2 min, a double emerged at 5.20 ppm, which could be ascribed to the protons in newly formed cyclobutane. Meanwhile, the new peaks at 6.93, 7.11, and 7.60 ppm ascribed to the protons in the photodimerization product (named as **D-BTAF24**) were also detected. The similar ^{1}H NMR spectral changes of **BTAF4** were observed during the UV irradiation of the microcrystals (Supporting Information Figure S8). This suggested that photodimerization was also the driving force for the transformation from light into mechanical energy in crystals of **BTAF4** and **BTAF24**.

To further demonstrate the driving force of the photomechanical behavior of the crystals, we collected the single-crystal data of **BOAF4**, **BOAF24**, **BTAF4**, and **BTAF24** as well as their dimers of **D-BOAF4**, **D-BOAF24** (α- and β-types), **D-BTAF4**, and **D-BTAF24**. Among them, the single-crystal structures of **BOAF4**, **BOAF24**, **D-BOAF4**, and **D-BOAF24** (α- and β-types) had been reported in our previous work.[42] Notably, Schmidt[52] found that the distance of "olefin pair" (<4.2 Å) as well as the angles of θ_2 and θ_3 (close to 90°) depicted in Supporting Information Chart S1 were geometric criteria for photodimerization. In the single crystal of **BOAF4**, the distance in "olefin pair" was 3.896 and 3.681 Å (Supporting Information Figure S9a), and θ_2 and θ_3 were ca. 77.00°/69.99° and 87.97°/83.04°, respectively (Supporting Information Table S3). Therefore, such molecular packing made the photodimerization of **BOAF4** accessible. Subsequently, the single-crystal structure of **D-BOAF4** was analyzed. For **D-BOAF4**, isomers I and II were achieved via photocycloaddition (Supporting Information Figure S9b). Taking isomer I as an example, the bond lengths of the newly formed C–C bond in the four-membered ring were 1.578 and 1.579 Å. Therefore, each carbon atom in the original C=C had to move ca.

DOI: 10.31635/ccschem.020.202000350
CCS Chem. **2020**, *2*, 1491–1500

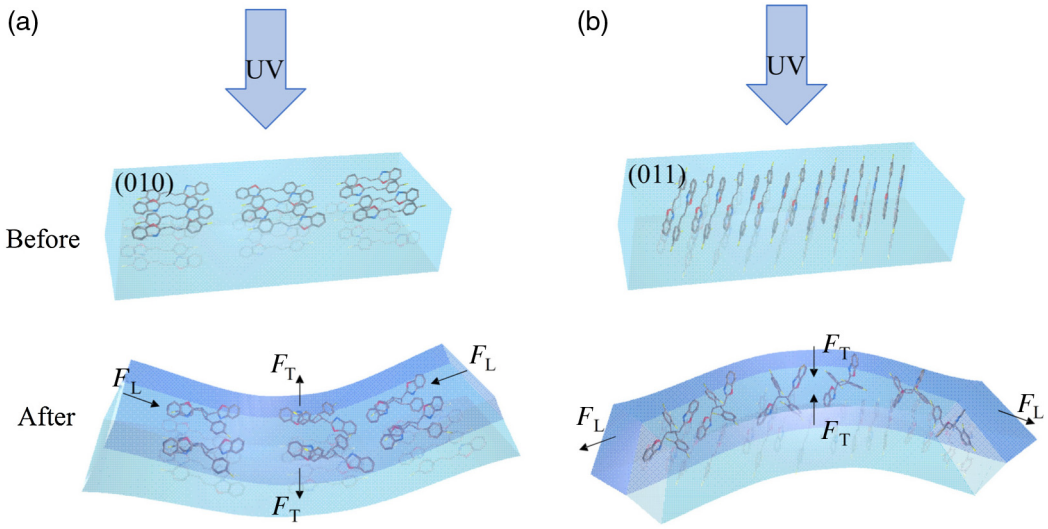

Figure 4. | *Schematic illustration of the bending of (a)* ***BOAF4*** *and (b)* ***BOAF24*** *under UV irradiation.*

1.1–1.3 Å during photodimerization. Meanwhile, the newly formed cyclobutane impelled the benzoxazole and benzene to move away from the four-membered ring, like a bird spreads its wings. As a result, the distances between the outermost F and C atoms reached 7.132 and 7.811 Å. Similar results were found from the single-crystal structures of **BOAF24**, **BTAF4**, and **BTAF24** (Supporting Information Figures S9b, S10, and S11). Since the molecular volume was amplified upon dimerization, the strain was yielded, leading to the mechanical movements of crystals.

More interestingly, based on the single crystal of **BOAF24**, it seems that [2 + 2] cycloaddition will yield only β-type dimer, but α-type **D-BOAF24** was also obtained (Supporting Information Figure S9b). The ratio of the amount of β- and α-type **D-BOAF24** was about 20:1 via column chromatography. Since **BOAF24** molecules were arranged in a head-to-head packing in the crystal, the β-type **D-BOAF24** was the main product as a dynamic product.[53] The possible reason for the formation of α-type **D-BOAF24** was shown in Supporting Information Figure S12. Under UV irradiation, molecules 1 and 2 are unparalleled and far from each other at the distance of 8.513 Å. However, the strains generated by [2 + 2] cycloaddition of other molecules satisfied with Schmidt's criteria squeezed the distance between molecules 1 and 2, thus affording α-type **D-BOAF24**. On the contrary, the dimerization of **BOAF4**, **BTAF4**, and **BTAF24** was only concerned with the prearrangement of the molecules with the distance <4.2 Å for "olefin pairs" in crystals.

It is time to discuss why **BOAF4** and **BTAF4** bent toward UV light, while **BOAF24** and **BTAF24** exhibited backlight bending performance. In 2003, Ikeda et al.[54] and Yu et al.[55] found that monodomain and polydomain liquid crystal elastomer (LCE) films showed different light-induced bending behavior, and the monodomain LCE bent along the alignment direction of the azobenzene mesogens., In 2006, they found that the initial alignment of photoactive mesogens significantly affected the bending behavior of the LCE films: the homogeneous films bent toward the irradiation direction of the actinic UV light, while the homotropic films bent away from the light source.[56] Thus, we proposed that the arrangement of molecules in the crystal has a crucial impact on the bending behavior.

First, it was proven that the strain would be generated from the phototropic surface of the crystal under the UV irradiation.[57] As shown in Figure 4a, the [2 + 2] cycloaddition mainly occurred on the (010) face of the crystal of **BOAF4**, which was the largest superficial area. Before UV irradiation, the molecules were longitudinally aligned along the long axis of the crystal. The molecular length decreased from 12.268 (**BOAF4**) to ca. 11.091 Å (the average value of the two isomers of **D-BOAF4** upon photodimerization). However, the molecular width of **D-BOAF4** was increased from 3.56 (the average value of the distance of two **BOAF4** molecules) to ca. 7.476 Å. Hence, on the (010) face of the **BOAF4** crystal, the force along the longitudinal direction (F_L) made the crystal shrink, while the force along the transverse direction (F_T) lead to the crystal's expansion. Therefore, on the (010) face of the crystal was extended along the transverse direction, while F_L compressed it in the longitudinal direction. As a result, the crystals of **BOAF4** exhibited phototropic bending behavior. Similarly, the [2 + 2] cycloaddition reaction of **BOAF24** took place on the (011) face of the crystal, leading to the decrease of the molecular length from 12.286 to 11.046 Å (the average value of β-type **D-BOAF24**) and the increase of the molecular width from an average of 3.863 to 6.822 Å (the average width of β-type **D-BOAF24**). However, the molecular alignment of **BOAF24** was different from that of **BOAF4**

DOI: 10.31635/ccschem.020.202000350
CCS Chem. **2020**, *2*, 1491–1500

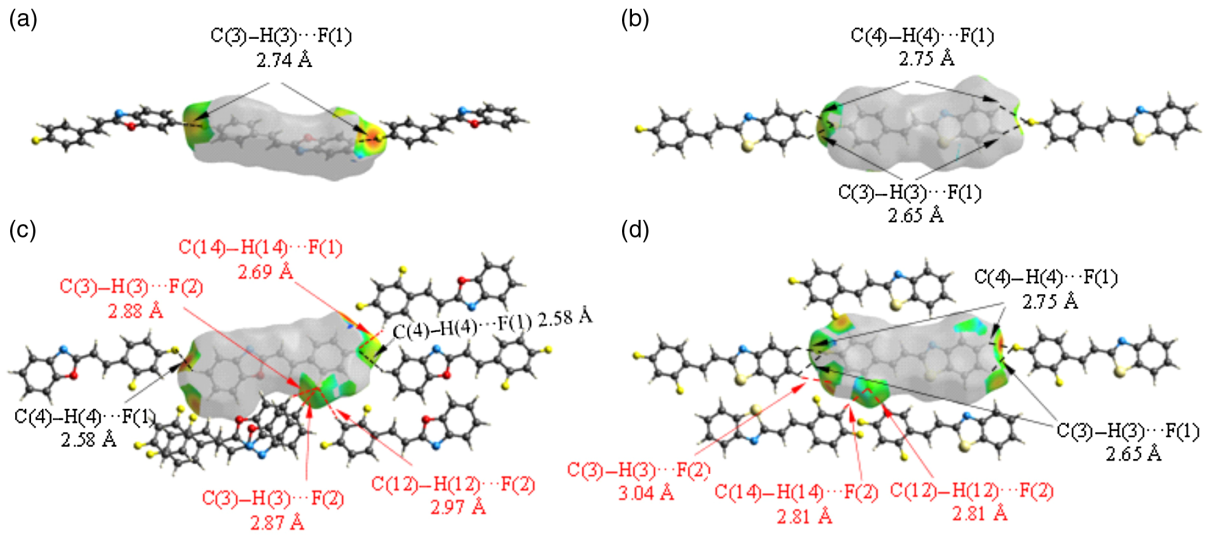

Figure 5. | *The Hirshfeld surfaces (mapped over* d_i*) and the distances of F···H–C interaction of (a)* ***BOAF4****, (b)* ***BTAF4****, (c)* ***BOAF24****, and (d)* ***BOAF24****.*

in crystal. Molecules of **BOAF24** aligned perpendicularly to the long axis of the crystal (Figure 4b). On the (011) face, the crystal was compressed along the transverse direction and extended along the longitudinal direction, exhibiting backlight bending behavior. Similar observations were also found for **BTAF4** and **BTAF24**.

Theoretical calculations

To investigate the different molecular packing within crystals, Hirshfeld surface and two-dimensional (2D) fingerprint plots of crystal stacking based on F···H–C interaction in crystals of **BOAF4**, **BOAF24**, **BTAF4**, and **BOAF24** were initially calculated (Supporting Information Figure S13). For **BOAF4**, there was only one kind of H-bond of C(3)–H(3)···F(1) with a distance of 2.74 Å, and the F···H–C interaction (the colored part in Figure 5a) makes the molecule align along the long axis of the crystal. However, except for the similar H-bond of C(4)–H(4)···F(1) (2.69 Å), four additional H-bonds of C(14)–H(14)···F(1) (2.69 Å), C(3)–H(3)···F(2) (2.88 Å), C(3)–H(3)···F(2) (2.87 Å), and C(12)–H(12)···F(2) (2.97 Å) were formed in the crystal of **BOAF24**. Besides, the Hirshfeld surface map based on **BOAF24** shows that the F···H–C interaction tends to form a plane (Figure 5c). Thus, the multiple H-bonds induced the molecules to align perpendicularly to the long axis of the crystal. Furthermore, F···H–C interactions in **BOAF24** account for 23.0% of the total intermolecular interactions, which is twice as much as that of **BOAF4** (12.2%) (Supporting Information Table S8). Therefore, we believe that the F···H–C interaction plays a key role in the different molecular packing in the crystals. The analysis of F···H–C interactions in the single crystals of **BTAF4** and **BTAF24** suggested similar results to those of **BOAF4** and **BOAF24** (Figures 5b and 5d).

To explore the mechanical properties of crystals, theoretical calculations were carried out with the density functional theory using the VASP software. Calculations of the elastic properties of crystals were conducted by imposing small strains along a specific direction to obtain the stiffness tensor. As listed in Supporting Information Table S9, the Pugh ratios obtained for the crystals of **BOAF4**, **BOAF24**, **BTAF4**, and **BTAF24** were 2.7280, 2.1115, 2.2372, and 1.9556, respectively. All of the values were larger than 1.75, indicating that they were elastic.[58] Moreover, it was observed that the Young's modulus of the phototropic surfaces of crystal **BOAF4**, **BOAF24**, **BTAF4**, and **BTAF24** were 3.06, 7.32, 6.02, and 4.05 GPa, respectively (Supporting Information Figures S14–S17). Thus, all the crystals were relatively easy to bend on the phototropic surface.

On the other hand, it was found that the modes of movement were related to the shapes of the dynamic molecular crystals. Crystals with a high length/diameter ratio were normally soft and flexible, and the needle-like crystals bent under the UV irradiation because the strain was released slowly. In the case of the block or slice-like crystal, the photodimerization took place on the large lateral area, yielding strong strain. When the rigid crystals could not withstand the colossal strain, they exploded rapidly and showed swinging or jumping behavior.[41]

Applications

To demonstrate the intrinsic potential of these photoactuators, a pushing experiment was performed on a glass substrate. Considering the high Young's modulus, the **BOAF24** crystal was chosen as a representative. As shown in Supporting Information Figure S18, a piece of cotton was adhered to the end of the rod-like crystal of

DOI: 10.31635/ccschem.020.202000350
CCS Chem. **2020**, *2*, 1491–1500

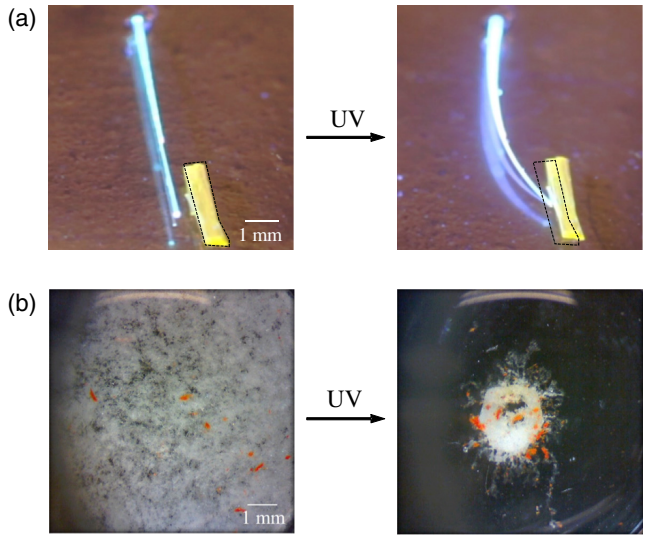

Figure 6. | *(a) Movement of a yellow organic crystal pushed by the rod-like crystal of **BOAF24** on UV irradiation (the dotted lines depict the edge of the crystal before irradiation). (b) The nanofibers of **BOAF24** shrink and enrich the pollutants under the UV irradiation.*

BOAF24. Upon UV irradiation, the crystal bent away from the light source with the cotton for about 0.2 mm, indicating that the crystal had sufficient actuation power to push objects. To further evaluate the capability of the actuator, a much heavier organic crystal was employed. As presented in Figure 6a and Supporting Information Video S12, the organic crystal was pushed away from its original position at about 0.3 mm under UV irradiation. Thus, it suggested that the **BOAF24** crystal, as a photoactuator, can perform mechanical work.

Except for pushing weights, fibers formed from **BOAF24** in an aqueous medium can grab undissolved objects. As shown in Figure 6b and Supporting Information Video S13, upon UV irradiation, **BOAF24** fibers began to shrink and then assemble into a small ball. Meanwhile, they gradually seized the organic compound dispersed in water and finally collected it into a small ball. A possible working mechanism is proposed below. In water, the fibers arranged very loosely and intertwined with each other due to the poor solubility. [2 + 2] Cycloaddition took place upon UV irradiation, which made the fibers initially bend, curve, and knot, and finally assemble into the small ball. Therefore, besides working as a conventional actuator, **BOAF24** has the potential to remove undissolved pollutants from water.

Conclusion

Styrylbenzoxazoles-based (**BOAF4** and **BOAF24**) and styrylbenzothiazoles-based (**BTAF4** and **BTAF24**) molecular crystals exhibited photosalient properties. Unexpectedly, **BOAF4** and **BTAF4** crystals exhibited bending behavior toward UV light, whereas **BOAF24** and **BTAF24** crystals showed negative phototropism behavior. This interesting phenomenon is due to different molecular packing resulting from different F···H–C interactions in the crystals. In detail, the F···H–C interactions of **BOAF4** and **BTAF4** crystals are linearly extensive, whereas the F···H–C interactions of **BOAF24** and **BTAF24** crystals have multiple directions. The different bending behaviors resulting from minor changes in molecular structure give us a new inspiration to design new photosalient crystals. This is the first report on exploring the relationship between the bending behavior and the molecular packing in organic crystals caused by [2 + 2] cycloaddition. Moreover, we obtained the physical properties of the crystals by theoretical calculation and found that they are elastic, which is a simple way to evaluate the mechanical properties of crystals. Taking advantage of this photoresponsive property, we achieved the potential application in pushing objects, as well as enriching and removing pollutants. Herein, we proposed and achieved varying photoresponsive behaviors of elastic crystals by molecular design, which opens a novel gate for crystal engineering.

Supporting Information

Supporting Information is available.

Conflict of Interest

There is no conflict of interest to report.

Preprint Acknowledgement

Research presented in this article was posted on a preprint server prior to publication in CCS Chemistry. The corresponding preprint article can be found here: https://doi.org/10.26434/chemrxiv.12413459.v1.

Acknowledgments

The authors are grateful for financial support from the National Science Foundation of China (nos. 51773067 and 21788102), the Open Project of State Key Laboratory of Supramolecular Structure and Materials (no. sklssm202019), the Research Grants Council of Hong Kong (no. C6009-17G), the Innovation of Technology Commission (no. ITC-CNERC14SC01), and the National Key Research and Development Program of China (no. 2018YFE0190200).

References

1. Sakai T.; Kagawa T.; Kasahara M.; Swartz T. E.; Christie J. M.; Briggs W. R.; Wada M.; Okada K. nph1 and npl1: Blue Light Receptors that Mediate Both Phototropism and

Chloroplast Relocation. *Proc. Natl. Acad. Sci. U. S. A*. **2001**, *98*, 6969–6974.
2. Atamian H. S.; Creux N. M.; Brown E. A.; Garner A. G.; Blackman B. K.; Harmer S. L. Circadian Regulation of Sunflower Heliotropism, Floral Orientation, and Pollinator Visits. *Science* **2016**, *353*, 587–590.
3. Dietrich D.; Pang L.; Kobayashi A.; Fozard J. A.; Boudolf V.; Bhosale R.; Antoni R.; Nguyen T.; Hiratsuka S.; Fujii N.; Miyazawa Y.; Bae T.-W.; Wells D. M.; Owen M. R.; Band L. R.; Dyson R. J.; Jensen O. E.; King J. R.; Tracy S. R.; Sturrock C. J.; Mooney S. J.; Roberts J. A.; Bhalerao R. P.; Dinneny J. R.; Rodriguez P. L.; Nagatani A.; Hosokawa Y.; Baskin T. I.; Pridmore T. P.; De Veylder L.; Takahashi H.; Bennett M. J. Root Hydrotropism Is Controlled via a Cortex-Specific Growth Mechanism. *Nat. Plants*. **2017**, *3*, 17057.
4. Medishetty R.; Husain A.; Bai Z.; Runcevski T.; Dinnebier R. E.; Naumov P.; Vittal J. J. Single Crystals Popping Under UV Light: A Photosalient Effect Triggered by a [2+2] Cycloaddition Reaction. *Angew. Chem. Int. Ed*. **2014**, *53*, 5907–5911.
5. Nath N. K.; Runcevski T.; Lai C. Y.; Chiesa M.; Dinnebier R. E.; Naumov P. Surface and Bulk Effects in Photochemical Reactions and Photomechanical Effects in Dynamic Molecular Crystals. *J. Am. Chem. Soc*. **2015**, *137*, 13866–13875.
6. Naumov P.; Chizhik S.; Panda M. K.; Nath N. K.; Boldyreva E. Mechanically Responsive Molecular Crystals. *Chem. Rev*. **2015**, *115*, 12440–12490.
7. Zhang L.; Naumov P. Light- and Humidity-Induced Motion of an Acidochromic Film. *Angew. Chem. Int. Ed*. **2015**, *54*, 8642–8647.
8. Wani O. M.; Zeng H.; Priimagi A. A Light-Driven Artificial Flytrap. *Nat. Commun*. **2017**, *8*, 15546.
9. Vale R. D.; Milligan R. A. The Way Things Move: Looking Under the Hood of Molecular Motor Proteins. *Science* **2000**, *288*, 88–95.
10. Chen J.; Leung F. K.; Stuart M. C. A.; Kajitani T.; Fukushima T.; van der Giessen E.; Feringa B. L. Artificial Muscle-Like Function from Hierarchical Supramolecular Assembly of Photoresponsive Molecular Motors. *Nat. Chem*. **2018**, *10*, 132–138.
11. Wie J. J.; Shankar M. R.; White T. J. Photomotility of Polymers. *Nat. Commun.* **2016**, *7*, 13260.
12. Ma Z. C.; Zhang Y. L.; Han B.; Liu X. Q.; Zhang H. Z.; Chen Q. D.; Sun H. B. Femtosecond Laser Direct Writing of Plasmonic Ag/Pd Alloy Nanostructures Enables Flexible Integration of Robust SERS Substrates. *Adv. Mater. Technol*. **2017**, *2*, 1600270.
13. Kobatake S.; Takami S.; Muto H.; Ishikawa T.; Irie M. Rapid and Reversible Shape Changes of Molecular Crystals on Photoirradiation. *Nature* **2007**, *446*, 778.
14. Panda M. K.; Ghosh S.; Yasuda N.; Moriwaki T.; Mukherjee G. D.; Reddy C. M.; Naumov P. Spatially Resolved Analysis of Short-Range Structure Perturbations in a Plastically Bent Molecular Crystal. *Nat. Chem.* **2015**, *7*, 65–72.
15. Kim T.; Al-Muhanna M. K.; Al-Suwaidan S. D.; Al-Kaysi R. O.; Bardeen C. J. Photoinduced Curling of Organic Molecular Crystal Nanowires. *Angew. Chem. Int. Ed.* **2013**, *52*, 6889–6893.
16. Koshima H.; Matsuo R.; Matsudomi M.; Uemura Y.; Shiro M. Light-Driven Bending Crystals of Salicylidenephenylethylamines in Enantiomeric and Racemate Forms. *Cryst. Growth Des.* **2013**, *13*, 4330–4337.
17. Bushuyev O. S.; Tomberg A.; Friscic T.; Barrett C. J. Shaping Crystals with Light: Crystal-to-Crystal Isomerization and Photomechanical Effect in Fluorinated Azobenzenes. *J. Am. Chem. Soc.* **2013**, *135*, 12556–12559.
18. Nath N. K.; Pejov L.; Nichols S. M.; Hu C.; Saleh N.; Kahr B.; Naumov P. Model for Photoinduced Bending of Slender Molecular Crystals. *J. Am. Chem. Soc.* **2014**, *136*, 2757–2766.
19. Ohshima S.; Morimoto M.; Irie M. Light-Driven Bending of Diarylethene Mixed Crystals. *Chem. Sci.* **2015**, *6*, 5746–5752.
20. Kitagawa D.; Tanaka R.; Kobatake S. Photoinduced Stepwise Bending Behavior of Photochromic Diarylethene Crystals. *Crystengcomm* **2016**, *18*, 7236–7240.
21. Koshima H.; Uchimoto H.; Taniguchi T.; Nakamura J.; Asahi T.; Asahi T. Mechanical Motion of Molecular Crystals Induced by [4+4] Photodimerisation. *Crystengcomm* **2016**, *18*, 7305–7310.
22. Al-Kaysi R. O.; Tong F.; Al-Haidar M.; Zhu L.; Bardeen C. J. Highly Branched Photomechanical Crystals. *Chem. Commun.* **2017**, *53*, 2622–2625.
23. Hirano A.; Hashimoto T.; Kitagawa D.; Kono K.; Kobatake S. Dependence of Photoinduced Bending Behavior of Diarylethene Crystals on Ultraviolet Irradiation Power. *Cryst. Growth Des.* **2017**, *17*, 4819–4825.
24. Kitagawa D.; Kawasaki K.; Tanaka R.; Kobatake S. Mechanical Behavior of Molecular Crystals Induced by Combination of Photochromic Reaction and Reversible Single-Crystal-to-Single Crystal Phase Transition. *Chem. Mater.* **2017**, *29*, 7524–7532.
25. Cheng S.-C.; Chen K.-J.; Suzaki Y.; Tsuchido Y.; Kuo T.-S.; Osakada K.; Horie M. Reversible Laser-Induced Bending of Pseudorotaxane Crystals. *J. Am. Chem. Soc.* **2018**, *140*, 90–93.
26. Samanta R.; Ghosh S.; Devarapalli R.; Reddy C. M. Visible Light Mediated Photopolymerization in Single Crystals: Photomechanical Bending and Thermomechanical Unbending. *Chem. Mater.* **2018**, *30*, 577–581.
27. Peng J.; Ye K.; Liu C.; Sun J.; Lu R. The Photomechanic Effects of the Molecular Crystals Based on 5-chloro-2-(naphthalenylvinyl)benzoxazols Fueled by Topo-Photochemical Reactions. *J. Mater. Chem. C* **2019**, *7*, 5433–5441.
28. Liu J.; Ye K.; Shen Y.; Peng J.; Sun J.; Lu R. Photoactuators Based on the Dynamic Molecular Crystals of Naphthalene Acrylic Acids Driven by Stereospecific [2+2] Cycloaddition Reactions. *J. Mater. Chem. C* **2020**, *8*, 3165–3175.
29. Peng J.; Ye K.; Yue Y.; Liu C.; Sun J.; Lu R. Photomechanical Effects of Acidochromic Diarylethene Derivatives. *Sci. Sin. Chim.* **2020**, *50*, 108–117.
30. Uchida K.; Sukata S.-i.; Matsuzawa Y.; Akazawa M.; de Jong J. J. D.; Katsonis N.; Kojima Y.; Nakamura S.; Areephong J.; Meetsma A.; Feringa B. L. Photoresponsive Rolling and

DOI: 10.31635/ccschem.020.202000350
CCS Chem. **2020**, *2*, 1491–1500

Bending of Thin Crystals of Chiral Diarylethenes. *Chem. Commun.* **2008**, 326–328.
31. Shtukenberg A. G.; Freudenthal J.; Kahr B. Reversible Twisting During Helical Hippuric Acid Crystal Growth. *J. Am. Chem. Soc.* **2010**, *132*, 9341–9349.
32. Kitagawa D.; Nishi H.; Kobatake S. Photoinduced Twisting of a Photochromic Diarylethene Crystal. *Angew. Chem. Int. Ed.* **2013**, *52*, 9320–9322.
33. Natarajan A.; Tsai C. K.; Khan S. I.; Mccarren P.; Houk K. N.; Garcia-Garibay M. A. The Photoarrangement of Alpha-Santonin Is a Single-Crystal-to-Single-Crystal Reaction: A Long Kept Secret in Solid-State Organic Chemistry Revealed. *J. Am. Chem. Soc.* **2007**, *129*, 9846–9847.
34. Commins P.; Natarajan A.; Tsai C. K.; Khan S. I.; Nath N. K.; Naumov P.; Garciagaribay M. A. Structure–Reactivity Correlations and Mechanistic Understanding of the Photorearrangement and Photosalient Effect of α-Santonin and Its Derivatives in Solutions, Crystals, and Nanocrystalline Suspensions. *Cryst. Growth Des.* **2015**, *15*, 1983–1990.
35. Ghosh S.; Mishra M. K.; Ganguly S.; Desiraju G. R. Dual Stress and Thermally Driven Mechanical Properties of the Same Organic Crystal: 2,6-Dichlorobenzylidene-4-fluoro-3-Nitroaniline. *J. Am. Chem. Soc.* **2015**, *137*, 9912–9921.
36. Medishetty R.; Sahoo S. C.; Mulijanto C. E.; Naumov P.; Vittal J. J. Photosalient Behavior of Photoreactive Crystals. *Chem. Mater.* **2015**, *27*, 1821–1829.
37. Uchida E.; Azumi R.; Norikane Y. Light-Induced Crawling of Crystals on a Glass Surface. *Nat. Commun.* **2015**, *6*, 7310.
38. Gupta P.; Panda T.; Allu S.; Borah S.; Baishya A.; Gunnam A.; Nangia A.; Naumov P.; Nath N. K. Crystalline Acylhydrazone Photoswitches with Multiple Mechanical Responses. *Cryst. Growth Des.* **2019**, *19*, 3039–3044.
39. Gupta P.; Karothu D. P.; Ahmed E.; Naumov P.; Nath N. K. Thermally Twistable, Photobendable, Elastically Deformable, and Self-Healable Soft Crystals. *Angew. Chem. Int. Ed.* **2018**, *57*, 8498–8502.
40. Kitagawa D.; Tsujioka H.; Tong F.; Dong X.; Bardeen C. J.; Kobatake S. Control of Photomechanical Crystal Twisting by Illumination Direction. *J. Am. Chem. Soc.* **2018**, *140*, 4208–4212.
41. Wang H.; Chen P.; Wu Z.; Zhao J.; Sun J.; Lu R. Bending, Curling, Rolling, and Salient Behavior of Molecular Crystals Driven by [2+2] Cycloaddition of a Styrylbenzoxazole Derivative. *Angew. Chem. Int. Ed.* **2017**, *56*, 9463–9467.
42. Wang H.; Xing H.; Gong J.; Zhang H.; Zhang J.; Wei P.; Yang G.; Lam J. W. Y.; Lu R.; Tang B. Z. "Living" Luminogens: Light Driven ACQ-to-AIE Transformation Accompanied with Solid-State Actuation. *Mater. Horiz.* **2020**, *7*, 1566–1572.
43. Kresse G.; Furthmüller J. Efficient Iterative Schemes for Ab Initio Total-Energy Calculations Using a Plane-Wave Basis Set. *Phys. Rev. B* **1996**, *54*, 11169.
44. Kresse G.; Furthmüller J. Efficiency of Ab-Initio Total Energy Calculations for Metals and Semiconductors Using a Plane-Wave Basis Set. *Comput. Mater. Sci.* **1996**, *6*, 15–50.
45. Blöchl P. E. Projector Augmented-Wave Method. *Phys. Rev. B* **1994**, *50*, 17953–17979.
46. Perdew J. P.; Burke K.; Ernzerhof M. Perdew, Burke, and Ernzerhof Reply. *Phys. Rev. Lett.* **1998**, *80*, 891–891.
47. de Jong M.; Chen W.; Angsten T.; Jain A.; Notestine R.; Gamst A.; Sluiter M.; Krishna Ande C.; van der Zwaag S.; Plata J. J.; Toher C.; Curtarolo S.; Ceder G.; Persson K. A.; Asta M. Charting the Complete Elastic Properties of Inorganic Crystalline Compounds. *Sci. Data* **2015**, *2*, 150009.
48. Wang H.; Zhao J.; Yang G.; Zhang F.; Sun J.; Lu R. Diarylethene-Based Xerogels: The Fabrication of More Entangled Networks Driven by Isomerization and Acidofluorochromism. *Org. Biomol. Chem.* **2018**, *16*, 2114–2124.
49. Liu Z.; Zhou C.; Lei T.; Nan X.-L.; Chen B.; Tung C.-H.; Wu L.-Z. Aggregation-Enabled Intermolecular Photo[2+2]cycloaddition of Aryl Terminal Olefins by Visible-Light Catalysis. *CCS Chem.* **2020**, *2*, 582–588.
50. Li J.; Shen P.; Zhao Z.; Tang B. Z. Through-Space Conjugation: A Thriving Alternative for Optoelectronic Materials. *CCS Chem.* **2019**, *1*, 181–196.
51. Wei P.; Zhang J.-X.; Zhao Z.; Chen Y.; He X.; Chen M.; Gong J.; Sung H. H. Y.; Williams I. D.; Lam J. W. Y.; Tang B. Z. Multiple yet Controllable Photoswitching in a Single AIEgen System. *J. Am. Chem. Soc.* **2018**, *140*, 1966–1975
52. Schmidt G. Photodimerization in the Solid State. *Pure Appl. Chem.* **1971**, *27*, 647–678.
53. Jiang Y.; Wang C.; Rogers C. R.; Kodaimati M. S.; Weiss E. A. Regio- and Diastereoselective Intermolecular [2+2] Cycloadditions Photocatalysed by Quantum Dots. *Nat. Chem.* **2019**, *11*, 1034–1040.
54. Ikeda T.; Nakano M.; Yu Y.; Tsutsumi O.; Kanazawa A. Anisotropic Bending and Unbending Behavior of Azobenzene Liquid-Crystalline Gels by Light Exposure. *Adv. Mater.* **2003**, *15*, 201–205.
55. Yu Y.; Nakano M.; Ikeda T. Directed Bending of a Polymer Film by Light. *Nature* **2003**, *425*, 145–145.
56. Kondo M.; Yu Y.; Ikeda T. How Does the Initial Alignment of Mesogens Affect the Photoinduced Bending Behavior of Liquid-Crystalline Elastomers? *Angew. Chem. Int. Ed.* **2006**, *45*, 1378–1382.
57. Sun J.-K.; Li W.; Chen C.; Ren C.-X.; Pan D.-M.; Zhang J. Photoinduced Bending of a Large Single Crystal of a 1,2-Bis (4-pyridyl)ethylene-Based Pyridinium Salt Powered by a [2+2] Cycloaddition. *Angew. Chem. Int. Ed.* **2013**, *52*, 6653–6657.
58. Pugh S. F. XCII. Relations Between the Elastic Moduli and the Plastic Properties of Polycrystalline Pure Metals. *Lond. Edinb. Dubl. Phil. Mag. J. Sci.* **1954**, *45*, 823–843.

DOI: 10.31635/ccschem.020.202000350
CCS Chem. **2020**, *2*, 1491–1500